Journal of Metallurgy and Materials Science, Vol. 62, No. 3-4, July-December 2020, pp. 31-40
Printed in India, © NML, ISSN 0972-4257

Effect of dual crosslinking on physico-chemical properties of hydrogels prepared from chitosan and alginate

SANTANU GHOSH, PRITIRANJAN MONDAL, B. RATHINA VEL and KAUSHIK CHATTERJEE*
Department of Materials Engineering, Indian Institute of Science, C.V. Raman Avenue, Bangalore, Karnataka- 560012, India

Abstract : Hydrogels have established their utility in the field of biomedical science and technology including drug delivery and tissue engineering, among other applications. Crosslinking density critically affects the resultant physical property of the hydrogels. Here, we have successfully synthesized carboxymethylchitosan (CMC) and oxidized alginate (AA) from chitosan and sodium alginate, respectively. CMC and AA were used to fabricate CMC-AA-single network (CMC-AA-SNH) and CMC-AA-double network (CMC-AA-DNH) hydrogels. Crosslinking of CMC-AA-SNH was done by dynamic covalent bonding, that is, imine bond formation, whereas CMC-AA-DNH was crosslinked via covalent imine bond and Ca^{2+} mediated ionic interactions. Fourier transform infrared spectroscopy (FTIR) and proton nuclear magnetic resonance (^{1}H NMR) studies were employed to characterize the components of the hydrogels. Effect of dual crosslinking over the single crosslinked hydrogel was extensively analyzed by rheological studies. Scanning electron microscopy revealed that the CMC-AA-DNH was more densely packed with interconnected structure than CMC-AA-SNH. Swelling study demonstrated that the degree of swelling of CMC-AA-DNH was significantly less than CMC-AA-SNH due to more crosslinking density. Compressive mechanical test of the hydrogels further indicated that CMC-AA-DNH exhibits fracture stress of 79.5 kPa. These results indicate how the physical and mechanical properties of a polymeric hydrogel system can be tuned through control of crosslinking, which have important implications for the use of these gels for biomedical applications.

Keywords: *hydrogels; chitosan; alginate; covalent crosslinking; ionic crosslinking; biopolymers; biomaterials*

INTRODUCTION

Hydrogels have gained enormous interest owing to their potential in diverse fields of biomedical science including drug delivery, peptide delivery, gene delivery, and tissue engineering, etc. [1, 2, 3] Over the years, researchers have proposed various definitions of hydrogels [4]. The simplest definition of hydrogels is that they are cross-linked three-dimensional (3D) polymeric networks, which may contain one or more polymers and are capable of holding a large amount of water. Cross-linking of hydrogels is known to be an important parameter as it plays a critical role in determining their physical integrity, swelling, and stiffness as well as other properties such as release behavior and degradation. Hydrogels can be crosslinked by different methods including chemical (covalent conjugations, enzyme mediated crosslinking, etc.) and physical (hydrogen bond formation, ionic interaction, stereocomplex formation, etc.) cross-linking [5]. A higher cross-linking density typically yields a much stiffer hydrogel than the lower cross-linked one. However, the degree of cross-linking can be tailored and depends on the target applications.

Various biodegradable, non-toxic polymers such as chitosan [6], sodium alginate[7], kappa carrageenan [8], guar gum [9], and gelatin [10], etc., have been used to prepare hydrogels for diverse biomedical applications. Among them, chitosan, which is a partially deacetylated form of chitin, is widely used in the food industries and medical applications such as wound healing and tissue engineering owing to its favorable properties such as biocompatibility, biodegradability, and antibacterial activity [11]. Sodium alginate, another naturally-derived biopolymer, has drawn enormous interests as it possesses properties similar to chitosan and can readily interact with different divalent cations such as Ca^{2+}, Sr^{2+}, and Mg^{2+} etc. to form hydrogels through ionic cross-linking [12]. Till now, several studies have been reported, wherein both chitosan and sodium alginate were used to develop hydrogels for different biomedical applications [13, 14, 15].

*Corresponding Author E-mail: kchatterjee@iisc.ac.in,

Recently, injectable hydrogels have been drawing increasing attention owing to their ability to readily form hydrogels and ease of delivery [16]. However, mechanical properties of these hydrogels are a concern limiting their use when employed as tissue adhesives or scaffolds for soft tissue regeneration. Mismatch in the elastic modulus of the hydrogel and the target tissue can result in poor biological outcomes.[17] Cross-linking is an important paramaters as it determines the mechanical properties of the hydrogels. Several research studies have been reported with double network hydrogels to explore different biomedical applications [18, 19]. However, there are few studies that have systematically compared the difference between single network hydrogel (SNH) and double network hydrogels (DNH) for a given polymeric system. Thus, in this study, we aimed to develop single cross-linked hydrogel (CMC-AA-SNH) and double cross-linked hydrogel (CMC-AA-DNH) prepared using CMC and AA and evaluate the effect of the crosslinking on their rheological behavior, swelling, and mechanical properties.

MATERIALS AND METHODS

Materials

Chitosan and sodium alginate were purchased from Sigma-Aldrich. Monochloroacetic acid and sodium periodate was procured from SD Fine Chemicals. Solvents used for this work were all analytical grade.

Synthesis of carboxymethyl-chitosan (CMC)

CMC was synthesized according to Bukzem et al with slight modification[20]. Briefly, 2 g of chitosan was suspended in 20 ml of 4:1 v/v isopropanol: water containing 2.7 g of sodium hydroxide and stirred for 1 h. Next, 3 g of monochloroacetic acid dissolved in isopropanol (4 ml) was added dropwise into the mixture above with continuous stirring for 30 min and the final mixture was stirred for 4 h at 60^0C. Thereafter, the reaction was quenched by adding excess 70% ethanol and neutralized with glacial acetic acid followed by filtration. The solid mass was repeatedly washed with increased ethanol content (70%, 80%, 90%) and finally dried under vacuum for 24 h.

Synthesis of oxidized alginate (AA)

AA was synthesized by the oxidation of alginate [21]. Briefly, 1 g of sodium alginate was dissolved in 100 ml of deionized water with continuous stirring. Subsequently, 5 µM of sodium periodate was added to the mixture above and the stirring was continued for 6 h in the dark. 1.5 ml of ethylene glycol was used to quench the reaction followed by dialysis (3.5 kDa MWCO) against deionized water for 3 days with regular change of deionized water. Next, the dialyzed sample was freeze-dried to obtain dried AA as the final product. AA was stored in -20^0 C until use.

Preparation of Hydrogels

CMC and AA based SNH (CMC-AA-SNH) was prepared by mixing the 4.5% w/v aqueous solution of CMC and 20% w/v aqueous solution of AA at the ratio of 3:2 into a cylindrical mold at room temp. CMC and AA based DNH (CMC-AA-DNH) was prepared in a similar way where 20 nM of $CaCl_2$ solution was added additionally to introduce the second crosslinking. In both the cases, the inverted tube method was employed to determine the gelation time.

Chemical Characterization

The synthesized CMC and AA were characterized by Fourier transform infrared (FTIR) spectroscopy (Perkin-Elmer, USA) using attenuated total reflection (ATR) mode, where the spectra were recorded within the range 4000 to 650 cm^{-1} with 4 cm^{-1} resolutions and 32 consecutive scans. ^{1}H nuclear magnetic resonance (^{1}H NMR) was

also performed at 400 MHz to confirm the successful synthesis of CMC and AA using D_2O and tetramethylsilane (TMS) as solvent and internal standard, respectively. Moreover, both CMC-AA-SNH and CMC-AA-DNH hydrogels were characterized by FTIR analysis.

Swelling Study

Swelling study was done by immersing CMC-AA-SNH and CMC-AA-DNH hydrogels in PBS 7.4 at 37°C. Sample weight was measured at predetermined time points until it did not change any further. Triplicate samples of each type of hydrogel were used for each measurement. Swelling ratio was calculated by the following equation.

$$\text{Swelling ration} = \frac{W_t - W_i}{W_i}$$

Where, W_t and W_i are the weight of the hydrogel at individual time points and initial weight of the hydrogels, respectively.

Rheology study

The dynamic rheological behaviors, including dynamic frequency sweep, dynamic strain sweep and dynamic temperature sweep were studied using the Discovery Hybrid Rheometer (DHR-3 from TA Instruments) using cone and plate geometry (diameter 40 mm, angle: 40 degree geometry gap: 200 µm). The lower plate was a Peltier device with a specifically designed temperature control system and the upper plate was made of stainless steel. For each measurement, each sample was carefully loaded onto the Peltier plate and the upper plate was set at a desired distance above the Peltier plate. Thereafter, dynamic frequency and strain sweep samples were equilibrated without pre-shearing or oscillating for 2 min at 37°C before conducting the experiments. For the temperature sweep, the sample was equilibrated at 25°C for 2 min.

(i) Dynamic Strain sweep

Before the dynamic viscoelastic measurements, the dynamic strain sweep from 1 to 800% at a fixed angular frequency 10 rad s^{-1} was first performed to identify the linear viscoelastic region (LVR) in which the storage modulus is independent of the strain amplitude and the gel to sol transition point. 1% strain was selected for the low amplitude oscillation test to ensure that the dynamic oscillatory deformation of each sample was in the LVR.

(ii) Dynamic frequency sweep

Shear storage modulus (G') and loss modulus (G'') were measured as functions of angular frequency (ω) over the range of 0.01 to 100 rad s^{-1} at 1 % strain at 37° C. The loss tangent (tanδ) was calculated by the equation ($\tan \delta = G'/G''$) and plotted as function of angular frequency.

(iii) Dynamic temperature sweep

To test the temperature stability of the hydrogel samples, G' and G'' were measured through a heating process 25°C to 60°C at $\omega = 10$ rad s^{-1} and $\gamma = 1\%$. Heating rate was 5°C / min.

Scanning electron microscopy

Longitudinal and cross-sectional regions of CMC-AA-SNH and CMC-AA-DNH were imaged using a scanning electron microscope (SEM, Ultra55 FE-SEM Karl Zeiss by Karl Zeiss SEM). For SEM imaging, both the hydrogel samples were freeze-dried followed by immersion into liquid nitrogen for few seconds prior to cutting into desired sections. Before imaging, samples were sputter coated with gold.

Mechanical Characterization

Compressive mechanical properties of hydrogels were evaluated using cylinder-shaped hydrogels (diameter of 7 mm and height of 2 mm) using the micro-universal testing machine (Mecmesin). A load cell of 25 N was used at a constant displacement rate of 1 mm/min until fracture. Triplicates of each type of hydrogel were measured.

RESULTS AND DISCUSSION

CMC and AA synthesis and characterization

CMC and AA were synthesized from chitosan and sodium alginate, respectively, and characterized by FTIR and ^{1}H NMR spectroscopic techniques. Fig 1(a) shows the characteristic broad FTIR absorption peaks of chitosan at 3600 to 3100 cm^{-1} for O-H and N-H stretching. The C=O stretching could be observed at 1656 cm^{-1}. The peaks at 1560 cm^{-1} and 1368 cm^{-1} correspond to N-H angular deformation and symmetric deformation of CH_3, respectively. Absorption at 1068 cm^{-1} corresponds to the C-O stretch. The FTIR spectra of CMC (Fig 1(a)) indicates the presence of COO^- as an intense absorption spectrum at 1584 cm^{-1}. The absorption band at 1410 cm^{-1} is observed, which is attributed to the symmetric and asymmetric deformations of COO^-, respectively. These results are in agreement with previously published work of Bukzem et al [20] and confirmed the successful formation of CMC.

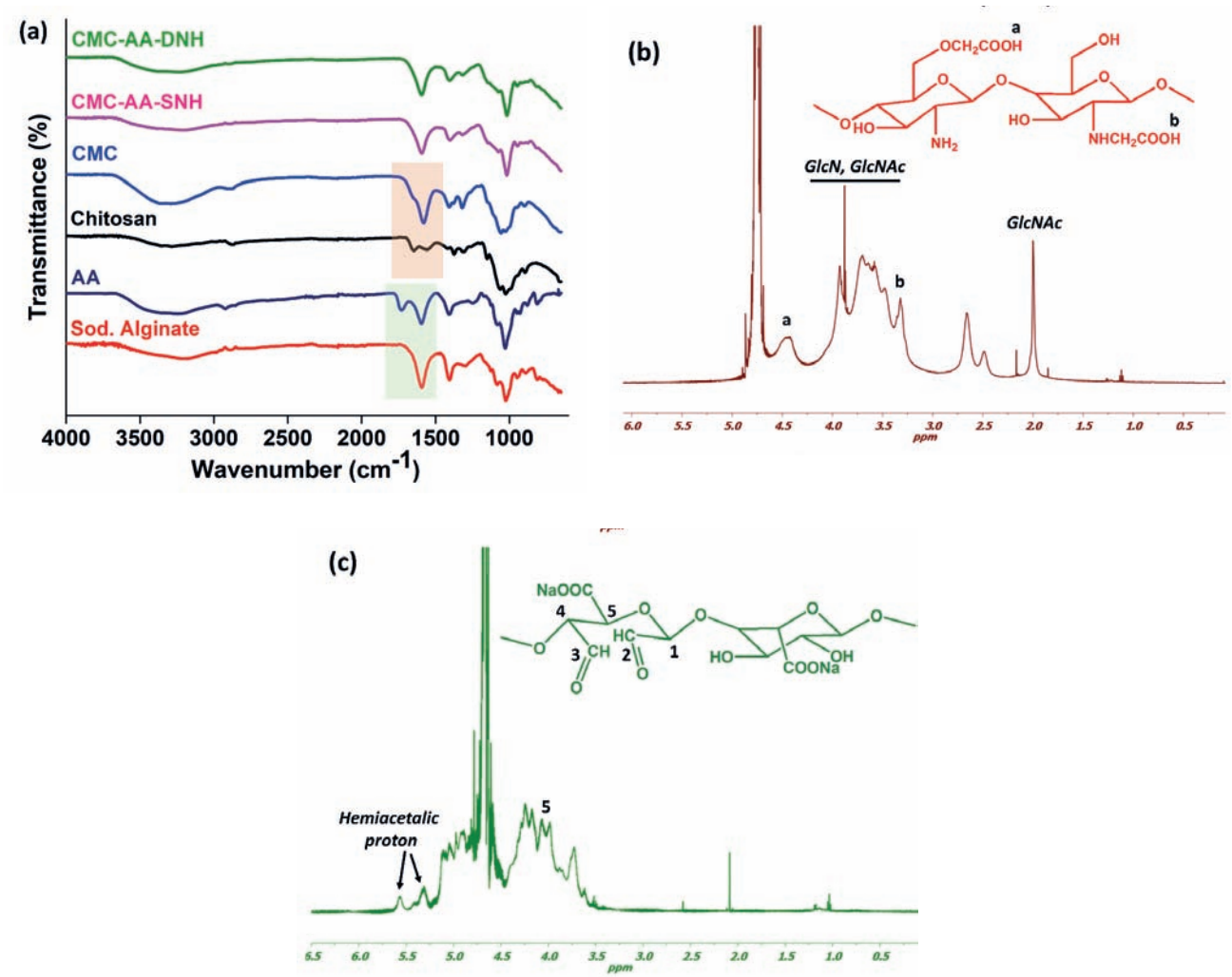

Fig 1. (a) FTIR spectra of sod. alginate, AA, chitosan, CMC, CMC-AA-SNH and CMC-AA-DNH; (b, c) 1H NMR spectra of (b) CMC and (c) AA.

The synthesis of CMC was further confirmed by ^{1}H NMR (Fig 1(b)). Chitosan is a copolymer, consisting of glucosamine (GlcN) and acetylglucosamine (GlcNAc) units. The characteristic methyl proton could be observed at 2.0 ppm, whereas peaks at the range of 3.4 to 4.1 ppm indicated the presence of hydrogens of GlcN and GlcNAc units. A broad peak at 4.3 to 4.6 ppm (a) is seen for the carboxymethyl protons and the adjacent protons of CH_2 indicating the O-carboxymethylation. Moreover, evidence of the formation of N-carboxymethylation could be observed as the peak around 3.3 ppm (b) indicated the protons of carboxymethyl group attached to nitrogen group of chitosan. [20]

Similarly, the formation of AA was confirmed by FTIR spectra (Fig 1(a)) and ^{1}H NMR spectra (Fig 1 (c)). Fig 1(a) presents the characteristic absorption spectrum of alginate. The broad peak at 3400 cm^{-1} indicates the O-H stretching vibration. The weak C-H stretching vibration could be observed at 2909 cm^{-1}. The asymmetric and symmetric stretching vibrations of COO^- could be found at 1596 cm^{-1} and 1404 cm^{-1}, respectively. All characteristic peaks could be observed for AA. However, a new absorption peak appeared around 1728 cm^{-1} that corresponds to the C=O stretching vibration of the aldehyde group, which indicated the formation of AA.[22] 1H NMR analysis further confirmed the formation of AA. Fig 1 (c) depicts the 1H NMR spectra of AA, where the appearance of two prominent signals at around 5.25 and 5.55 ppm indicate the presence of hemiacetalic protons, which formed from aldehyde and the neighbouring hydroxyl groups. Similar observations were reported by Gomez et al [23] and thus, corroborate the results presented here confirming the formation of AA.

Hydrogel formation and gelation time

Fig 2 (a) shows the schematic representation of hydrogel preparation for CMC-AA-SNH ad CMC-AA-DNH. Figs 2 (b) and (c) present the digital photographs of the two hydrogels formed in the vials. Schiff base chemistry was employed to develop CMC-AA-SNH, wherein the hydrogel was rapidly formed by the homogeneous mixing of aqueous CMC and AA solutions in proportions listed in Table 1. The amine groups of CMC readily reacted with the aldehyde group of AA to produce dynamic covalent imine bonds. Similarly, Schiff base chemistry was used to prepare CMC-AA-DNH hydrogels along with the introduction of a secondary crosslinker, i.e., Ca^{2+} ions at a predetermined concentration as listed in Table 1. Divalent Ca^{2+} ions rapidly reacted with the carboxylic acid groups of AA polymeric chains through ionic cross-linking. The resultant hydrogels were characterized by FTIR spectroscopy, which confirmed the formation of the imine bond in both hydrogels, as revealed by the absorption at around 1700 cm^{-1} (Fig 1(a)). The gelation time was calculated by tube inversion method for both CMC-AA-SNH and CMC-AA-DNH and is tabulated in Table 1. The gelation time of 20s for CMC-AA-SNH here is significantly faster than for similar hydrogels reported by others. For example, Lei et al [24] utilized the Schiff base reaction to prepare dynamic self-healing hydrogels from amino-gelatin and dialdehyde carboxymethyl cellulose with gelation time of approximately 2 h. Furthermore, the gelation time decreased to 10 s for CMC-AA-DNH (Table 1) indicating that the ionic bonds formed faster than the dynamic imine bonds.

Table 1. Composition of different hydrogels and their corresponding gelation time

	CMC (4.5% w/v): AA (20% w/v)	**$CaCl_2$ aqueous solution (nM)**	**Gelation time (s)**
CMC-AA-SNH	3:2	0	20
CMC-AA-DNH	3:2	20	10

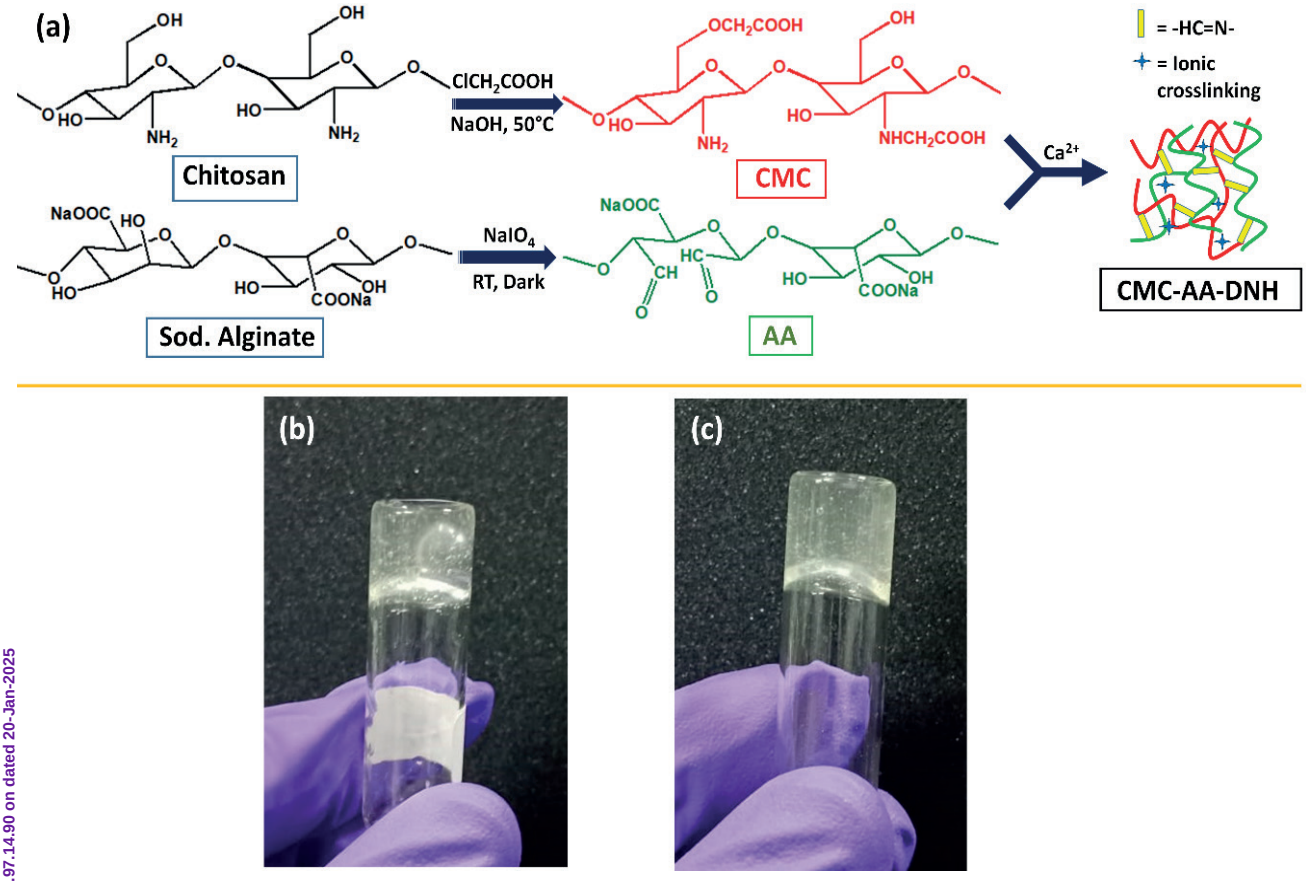

Fig 2. ***(a) Schematic representation of the CMC-AA-DNH gel formation; (b, c) Digital photographs of gels formed in inverted tubes of (b) CMC-AA-SNH and (c) CMC-AA-DNH.***

Rheological study

Fig 3(a) shows the G' and G'' as a function of % strain for both CMC-AA-SNH and CMC-AA-DNH hydrogels, which are the characteristic of the elastic response of hydrogels. In the LVR region, G' values of both hydrogels are essentially independent of the applied strain. The linear viscoelastic behavior deviated beyond a critical strain. The strain where the G' values of the hydrogels deviated by more than 5% from the linear region indicated the critical strains (γc) for each hydrogel [25]. Above γc, the G' values then rapidly decreased and crossed over the G'' plot indicating the gel-to-sol transition point (γt). This transition point indicates a transformation from the quasi-solid state to quasi-liquid sol state. As shown, in Table 2, The γc values of CMC-AA-SNH and CMC-AA-DNH hydrogels are 6.33 and 4.12 %, respectively. Therefore, γ = 1% was used for the subsequent low amplitude oscillation tests, The corresponding G'max of CMC-AA-SNH and CMC-AA-DNH are 289 Pa and 737 Pa, respectively (Table 2 and Fig 3 a). The G'max of CMC-AA-DNH is 2.5 times more than G'max of CMC-AA-SNH due to the addition of a small amount of Ca^{2+} ions. In the presence of Ca^{2+} ions, more chelation happened in the CMC-AA-DNH system and as a result, the viscoelasticity and stiffness of the CMC-AA-DNH increased noticeably compared to CMC-AA-SNH. It can be observed that CMM-AA-DNH presented a moderately higher G'max compared to CMC-AA-SNH, as well as shorter LVR window and therefore, lower γc. These observations indicate that CMC-AA-DNH was a much stiffer and stronger hydrogel than CMC-AA-SNH.

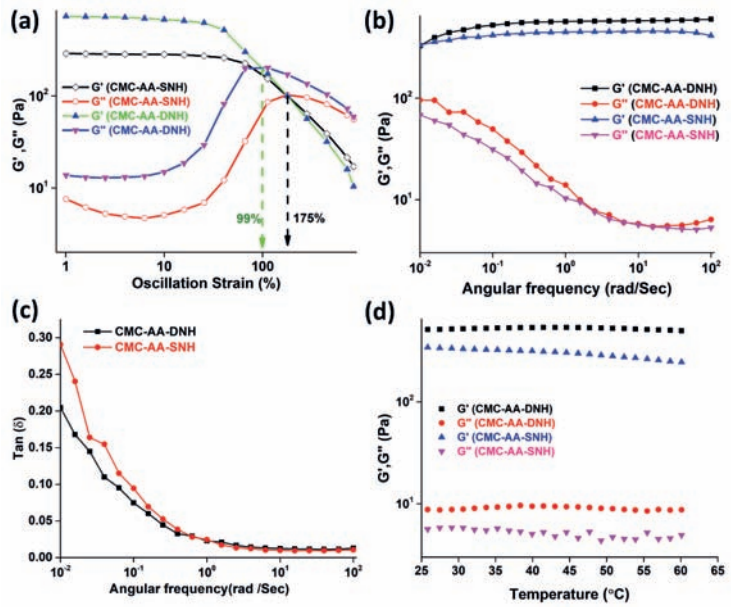

Fig 3. Dynamic viscoelasticity performance of both hydrogels at 37°C (a) The G' and G" of the hydrogel from strain amplitude sweep (γ = 1%–800%) at a fixed angular frequency (10 rad s-1) (b) Frequency dependence (0.01 to 100 rad s-1) of G' and G" at γ = 1% (c) frequency dependence of tan δ for both hydrogel (d) temperature dependence of G' and G" during heating (25 to 60° C, 5°C / min) at γ = 1% and ω = 10 rad s-1.

To understand the influence of Ca^{2+} ions on the viscoelastic properties of hydrogels, low amplitude oscillatory measurements were carried out at 37°C for CMC-AA-SNH & CMC-AA-DNH (Fig 3b). It can be seen that G'(ω) and G''(ω) of both hydrogels followed a similar trend. As ω increased, there is nearly a monotonic increase in G' and decrease in G'', which begins to suggest more entanglement network together with a strong elastic gel network. [26] Throughout the experimental frequency window (0.01 to 100 rad s^{-1}), G'is greater than G''and tan δ is also less than 1.0 (Fig 3c), which demonstrates the solid-like elastic behavior of hydrogels. This feature is consistent with the response observed typically for viscoelastic materials with a narrow distribution of relaxation time. [27] The marginal increase of moduli in CMC-AA-DNH is indicative of the rearrangement of Ca^{+2} ions to form higher-order network structure under shear stress. The magnitude of G'(ω) values of CMC-AA-DNH was more than the magnitude of G'(ω) values of CMC-AA-SNH in the measured window (0.01 to 100 rad s^{-1}), again signifying stronger gel-like behavior of CMC-AA-DNH due to the additional ionic crosslinking in the system resulting from the Ca^{2+} ions.

Table 2: Rheological characteristics of the hydrogels

Parameters	CMC-AA-SNH	CMC-AA-DNH
Critical Strains (γ_c) %	6.33	4.12
Transition point (γ_t) %	175	99
Maximum G' within LVR, G'_{max} (Pa)	289	737
Crossover modulus, G_c (Pa)	99	202

To understand the behavior of hydrogel with temperature, temperature sweep studies have been performed. Fig 3d shows the temperature dependence of moduli (G' and G'') for both hydrogels. Both hydrogels exhibited similar behavior. The moduli were nearly independent of temperature within the temperature range examined. G' of CMC-AA-SNH decreased marginally with an increase of temperature from 50° to 60°C, unlike the steady response of CMC-AA-DNH, which is suggestive of less stable crosslinking structure in CMC-AA-SNH than in CMC-AA-DNH.

SEM study

The surface morphology and internal structure of the lyophilized gels are shown in Fig 4(a) to (d). It was observed that both gels had a highly porous structure. The average pore size of CMC-AA-DNH (140 ± 32 µm, calculated from Fig 4a) was lower than the average pore size of CMC-AA-SNH (174 ± 39 µm, calculated from Fig 4c). This observation may be attributed to the fact that CMC-AA-DNH was stiffer and denser than the CMC-AA-SNH resulting from the higher crosslinking density in the presence of Ca^{2+} ions. From the micrograph of Fig 4b & 4d (longitudinal section of the sample), it was also observed that pores are highly interconnected. This interconnecting and irregular porous structure of 3D hydrogel is well suited for cell adhesion and proliferation.

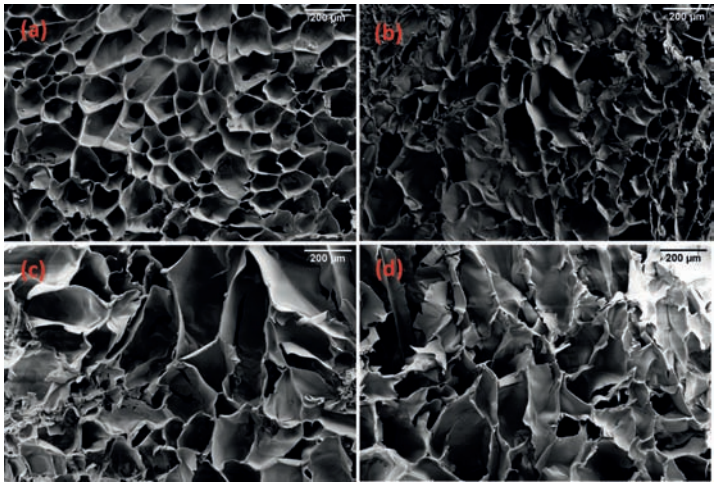

Fig 4. Scanning electron micrographs of (a) CMC-AA-DNH in cross-section, (b) CMC-AA-DNH in longitudinal direction, (c) CMC-AA-SNH in cross-section and (d) CMC-AA-SNH in longitudinal section.

Swelling study

The ability of the hydrogels for water uptake and resultant swelling was characterized for their use in biomedical applications. Fig 5 (a) compiles the swelling behavior of both hydrogels. CMC-AA-DNH almost reached equilibrium within 24 h and the swelling ratio was calculated to be 2.3. In contrast, CMC-AA-SNH swelled to reach equilibrium after 36 h and the swelling ratio was 5.5. This observation may be again being attributed to the fact that CMC-AA-DNH is relatively more tightly cross-linked than CMC-AA-SNH. When crosslinking density is less, the swelling swollen ratio is high. In CMC-AA-DNH, cross-linked density is more due to the additional Ca^{2+} -mediated ionic cross-linking.

Mechanical Property

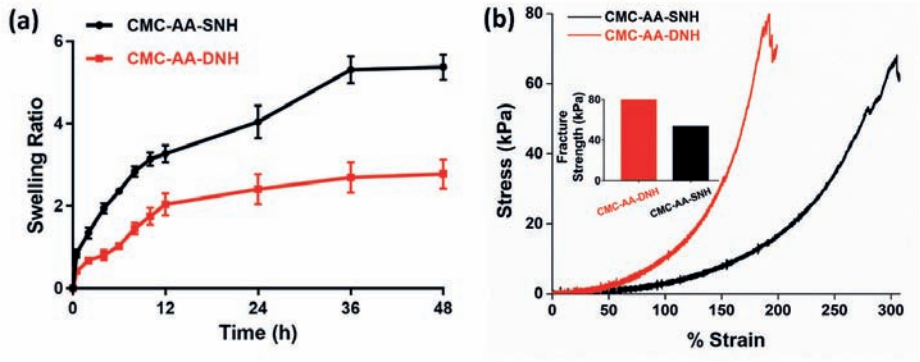

Fig 5. Comparative study of CMC-AA-SNH and CMC-AA-DNH (a) swelling, (b) compressive mechanical behavior

The mechanical properties of the hydrogels were assessed under compression. From the stress-strain curves in

Fig 5 (b), it is seen that CMC-AA-DNH exhibits higher modulus and maximum stress (79.5 kPa vs. 53.4 kPa) prior to failure but lower strain to failure (192% vs. 305%) than CMC-AA-SNH. These results are consistent with the data from rheology and a consequence of the increased cross-linking in CMC-AA-DNH compared to CMC-AA-DNH. Wei et al [21] also studied chitosan and alginate based hydrogels and the resulting hydrogel exhibited strength of 33 kPa. Lu et al [28] examined the effect of ionic concentration on dopamine modified 4 armed poly (ethylene glycol) hydrogel. They observed that the strength of the hydrogel was 65 kPa. In this work, we were able to achieve hydrogels with good strength by introduction of double network system using a combination of ionic and covalent bonding.

CONCLUSION

CMC and AA were synthesized and characterized by FTIR and ^{1}H NMR. Both pre-polymers were used to fabricate CMC-AA-SNH and CMC-AA-DNH hydrogels, where, CMC-AA-SNH was prepared by single covalent crosslinking whereas, covalent as well as ionic crosslinking were employed to prepare dual cross-linked CMC-AA-DNH. Faster gelation was observed for CMC-AA-DNH. Rheological properties were extensively studied for both the hydrogels and it was observed that CMA-AA-DNH is more viscoelastic as well as stiffer than CMC-AA-SNH. Denser and interconnected pores were observed for dual crosslinked CMC-AA-DNH hydrogel. Due to the higher crosslinking density, CMC-AA-DNH showed less swelling and higher strength than the single cross-linked CMC-AA-SNH hydrogel. It can be concluded that the presence of dual crosslinking CMC-AA-DNH yields much stiffer and stronger hydrogels than the single crosslinked CMC-AA-SNH. These results demonstrate how the physico-chemical properties of hydrogels derived from biopolymers may be tuned to meet the needs for different biomedical applications through careful selection of cross-links.

ACKNOWLEDGEMENTS

Funding from the Nanomission Programme of the Department of Science and Technology (DST), Government of India (Project DST/NM/NB/2018/119) is gratefully acknowledged. S.G. acknowledge SERB for the National Postdoctoral Fellowship (PDF/2019/000553). We thank Prof. Suryasarathi Bose for access to the rheometer.

DECLARATION

The authors declare no conflict of interest.

REFERENCES

[1] J. Li, D. J. Mooney: Designing hydrogels for controlled drug delivery. Nature Reviews Materials. 1: 1-7, 2016.

[2] N. Carballo-Pedrares, I. Fuentes-Boquete, S. Díaz-Prado, A. Rey-Rico: Hydrogel-Based Localized Nonviral Gene Delivery in Regenerative Medicine Approaches—An Overview. Pharmaceutics. 12: 752, 2020.

[3] S.H. Parekh, K. Chatterjee, S. Lin-Gibson, N.M. Moore, M.T. Cicerone, M.F. Young, C.G. Simon, Jr.: Modulus-driven differentiation of marrow stromal cells in 3D scaffolds that is independent of myosin-based cytoskeletal tension. Biomaterials. 32: 2256-2264, 2011.

[4] E.M. Ahmed: Hydrogel: Preparation, characterization, and applications: A review. Journal of Advanced Research 6: 105-121, 2015.

[5] W.E. Hennink, C.F. van Nostrum: Novel crosslinking methods to design hydrogels. Advanced drug delivery reviews. 64: 223-236, 2012.

[6] Z. Shariatinia, A.M. Jalali: Chitosan-based hydrogels: preparation, properties and applications. International journal of biological macromolecules. 115: 194-220, 2018.

[7] A.C. Hernández-González, L. Téllez-Jurado, L.M. Rodríguez-Lorenzo: Alginate hydrogels for bone tissue engineering, from injectables to bioprinting: A review. Carbohydrate Polymers. 229:115514, 2020.

[8] A. Rasool, S. Ata, A. Islam, R.U. Khan: Fabrication of novel carrageenan based stimuli responsive injectable hydrogels for controlled release of cephradine. RSC advances. 9: 12282-12290:2019.

[9] S. Das, U. Subuddhi: Guar gum–poly (N-isopropylacrylamide) smart hydrogels for sustained delivery of 5-fluorouracil. Polymer Bulletin. 76: 2945-2963, 2019.

[10] K. Dey, S. Agnelli, M. Serzanti, P. Ginestra, G. Scarì, P. Dell'Era, L. Sartore: Preparation and properties of high performance gelatin-based hydrogels with chitosan or hydroxyethyl cellulose for tissue engineering applications. International Journal of Polymeric Materials and Polymeric Biomaterials. 68: 183-192, 2019.

[11] P. Domalik-Pyzik, J. Chłopek, K. Pielichowska: Chitosan-based hydrogels: preparation, properties, and applications. Cellulose-Based Superabsorbent Hydrogels, MIH Mondal, Editor. 1665-1693, 2019.

[12] Q. Zhou, H. Kang, M. Bielec, X. Wu, Q. Cheng, W. Wei, H. Dai: Influence of different divalent ions cross-linking sodium alginate-polyacrylamide hydrogels on antibacterial properties and wound healing. Carbohydrate polymers. 197: 292-304, 2018.

[13] J. Chalitangkoon, M. Wongkittisin, P. Monvisade: Silver loaded hydroxyethylacryl chitosan/sodium alginate hydrogel films for controlled drug release wound dressings. International Journal of Biological Macromolecules. 159: 194-203, 2020.

[14] G. Wang, X. Wang, L. Huang: Feasibility of chitosan-alginate (Chi-Alg) hydrogel used as scaffold for neural tissue engineering: a pilot study in vitro. Biotechnology & Biotechnological Equipment. 31: 766-773, 2017.

[15] L. Xing, J. Sun, H. Tan, G. Yuan, J. Li, Y. Jia, D. Xiong, G. Chen, J. Lai, Z. Ling, Y. Chen: Covalently polysaccharide-based alginate/chitosan hydrogel embedded alginate microspheres for BSA encapsulation and soft tissue engineering. International journal of biological macromolecules. 127: 340-348, 2019.

[16] Y. Sun, D. Nan, H. Jin, X. Qu: Recent advances of injectable hydrogels for drug delivery and tissue engineering applications. Polymer Testing. 81: 106283, 2020.

[17] K. Chatterjee, S. Lin-Gibson, W.E. Wallace, S.H. Parekh, Y.J. Lee, M.T. Cicerone, M.F. Young, C.G. Simon, Jr.: The effect of 3D hydrogel scaffold modulus on osteoblast differentiation and mineralization revealed by combinatorial screening. Biomaterials 31: 5051-5062, 2010.

[18] M.A. Haque, T. Kurokawa , J.P. Gong: Super tough double network hydrogels and their application as biomaterials. Polymer. 53: 1805-1822, 2012.

[19] J.P. Gong: Why are double network hydrogels so tough?. Soft Matter. 6: 2583-2590, 2010.

[20] A.L. Bukzem, R. Signini, D.M. dos Santos, L. M. Lião, D.P. Ascheri: Optimization of carboxymethyl chitosan synthesis using response surface methodology and desirability function. International journal of biological macromolecules. 85: 615-624, 2016.

[21] Z. Wei, J.H. Yang, Z.Q. Liu, F. Xu, J. X. Zhou, M. Zrínyi, Y. Osada, Y.M. Chen: Novel biocompatible polysaccharide-based self-healing hydrogel. Advanced Functional Materials. 25: 1352-1359, 2015.

[22] M. Tian, X. Chen, H. Li, L. Ma, Z. Gu, X. Qi, X. Li, H. Tan, C. You: Long-term and oxidative-responsive alginate–deferoxamine conjugates with a low toxicity for iron overload. RSC advances. 6: 32471-32479, 2016.

[23] C.G. Gome, M. Rinaudo, M. A. Villar: Oxidation of sodium alginate and characterization of the oxidized derivatives. Carbohydrate Polymers. 67: 296-304, 2007.

[24] J. Lei, X. Li, S. Wang, L. Yuan, L. Ge, D. Li, C. Mu: Facile fabrication of biocompatible gelatin-based self-healing hydrogels. ACS Applied Polymer Materials. 1: 1350-1358, 2019.

[25] S. Gao, J. Guo, K. Nishinari: Thermoreversible konjac glucomannan gel crosslinked by borax. Carbohydrate Polymers. 72: 315-325, 2008.

[26] Y. Wang, L. Chen: Impacts of nanowhisker on formation kinetics and properties of all-cellulose composite gels. Carbohydrate Polymers. 83: 1937-1946, 2011.

[27] T. Inoue, K. Osaki: Rheological properties of poly(vinyl alcohol)/sodium borate aqueous solutions. Rheol Acta. 32: 550-555, 1993.

[28] L. Lu, T. Tian, S. Wu, T. Xiang, S. Zhou: A pH-induced self-healable shape memory hydrogel with metal-coordination cross-links. Polymer Chemistry. 10: 1920-1929, 2019.